

# EPA Particulate Matter Data - Analyses using Local Control Strategy

Robert L. Obenchain and S. Stanley Young

September 2022

## Abstract

Analyses of large observational datasets tend to be complicated and prone to fault depending upon the variable selection, data cleaning and analytic methods employed. Here, we discuss analyses of 2016 US environmental epidemiology data and outline some potential implications of our *Non-parametric and Unsupervised Learning* perspective. Readers are invited to download the CSV files we have contributed to **dryad** and apply the analytic approaches they think appropriate. We hope to encourage development of a broad-based “consensus view” of the potential effects of Secondary Organic Aerosols (Volatile Organic Compounds that have predominantly Biogenic or Anthropogenic origin) within PM<sub>2.5</sub> particulate matter on Circulatory and/or Respiratory mortality. The analyses described here ultimately focus on the question: “Is life in a region with relatively high air-borne Biogenic particulate matter also relatively dangerous in terms of Circulatory and/or Respiratory mortality?”

Keywords: Nonparametric Unsupervised Learning, Local Control Strategy, Clustering as Matching, Permutation Distributions.

## 1 Introduction

When a researcher starts analyzing a large cross-sectional dataset downloaded from the internet, it’s too late to worry about deficiencies in the *experimental design* characteristics of observational data! It is what it is. You could discard parts of the data to make the remainder “look better”: e.g. look more *blocked* and/or *balanced*. But using less than essentially “all” of the available data opens you up to accusations of “cherry-picking” or having “gardened” the data to get the answer you want, Glaeser (2006).

One sound approach is to use R-functions and CRAN-packages that implement a comprehensive and adaptive strategy that helps you to robustly “*design your analyses*” of potentially diverse and/or confounded measurements, as illustrated here using data from Pye et al. (2021). The approach illustrated here uses the *LocalControlStrategy* R-package of Obenchain (2015-2019).

The scatter plot in Figure 1 displays  $x = \text{Bvoc model predictions } (\mu\text{g}/\text{m}^3)$  from the EPA versus  $y = \text{AACRmort estimates from the CDC for 2,980 US Counties}$ . The Bvoc component of PM<sub>2.5</sub> consists of *volatile organic compounds* that are primarily Biogenic (rather than Anthropogenic) in origin within “Secondary Organic Aerosols”, Pye et al.

(2021). AACRmort values are “Age Adjusted Circulatory and/or Respiratory mortality” counts of deaths per 100,000 residents.

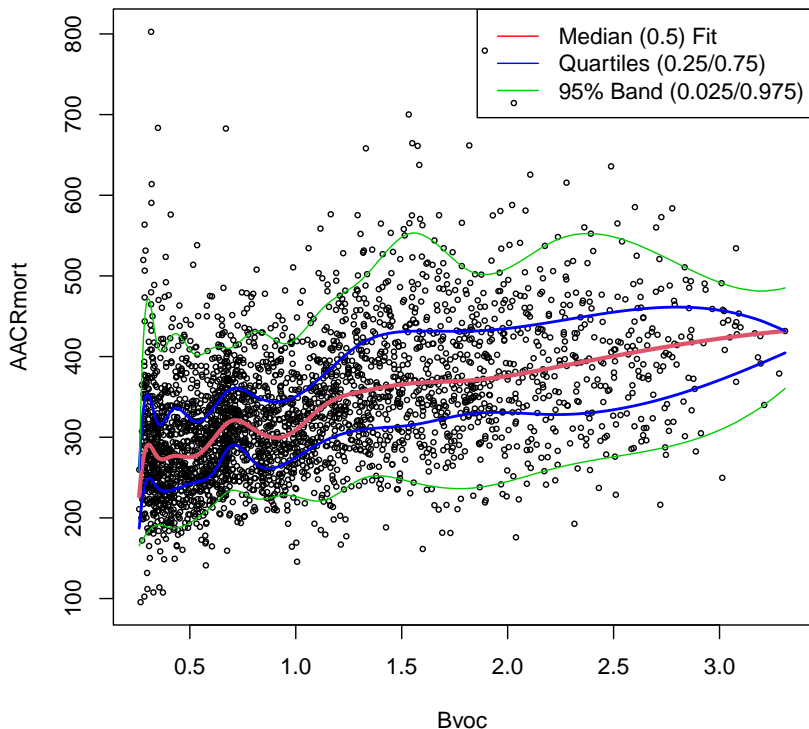


Figure 1: The above scatter for 2980 US Counties within the contiguous 48 States and Washington DC displays considerable variability in  $y = \text{AACRmort}$  for any given value of  $x = \text{Bvoc}$ . The five (red, blue or green) regression quantiles fitted using the quantreg  $R$ -package, Koenker (2005-2022), display considerable non-linearity. Thus, given only the Bvoc level of an otherwise unspecified US County, it would clearly be unrealistic to expect a meaningful point-prediction of its AACRmort count to result.

In natural products research, it is standard practice to examine fractions of raw natural material to figure out where an “active agent” is located. There typically are many fewer compounds in the active fraction, so chemical identification becomes more feasible. Starting in 1993, evidence pointing to particulate matter smaller than 2.5 microns, thereafter known as  $\text{PM}_{2.5}$ , became the proposed active fraction in the 1952 London Fog death event ...according to (unpublished) work by British environmentalists.

In reality,  $\text{PM}_{2.5}$  is a complex mixture of over four thousand chemical compounds which vary over both time and

space (urban vs. rural, etc.) Pye et al. (2021) appear to have followed a natural products strategy by arguing that “Secondary Organic Aerosols” (SOAs) could be “the” active agents in PM<sub>2.5</sub>. Unfortunately, in the almost 30 years since the first PM<sub>2.5</sub> publications sponsored by the US EPA, neither measures of PM<sub>2.5</sub> itself, nor any fraction of it, has been shown to be genuinely predictive of mortality at the level of individual US Counties or Cities.

Young, Kindzierski and Randall (2021) suggest that the current EPA paradigm that “PM<sub>2.5</sub> is, by itself, lethal” is wrong. While the efforts of Pye et al. (2021) may be noble, potential challenges to their proposals abound.

## 2 Predicted rather than Observed Measures of SOAs

Although actual measurements of SOA components in air samples are apparently not currently feasible, various “models” for predicting their presence from measurements of other pollutants have apparently been used since Volkamer et al. (2006). The analyses presented in Pye et al. (2021) appear to be based on EPA CMAQ models (2019), but Pye et al. (2021) do not discuss the assumptions or limitations of those models.

For example, a potential issue is that CMAQ methods may be loosely based upon Generalized Additive Model (GAM) concepts. While Pye et al. (2021) do reference Wood (2003,2004,2022), their introduction states “We use multiple linear regression...”. Since GAMs are a “composite” of individual models, some parts could be fit in unspecified “non-standard” ways. All that we know as outside observers is that their EPA models do a much better job of “predicting” CDC measures of Circulatory and Respiratory mortality (raw or age-adjusted) than we would have expected. In short, we would much rather have *actual “observed” measurements of secondary organic aerosols from validated scientific instruments* to contribute to **dryad** and analyze here.

### 2.1 Variables in the Data from the CDC, EPA & Other Federal Agencies

While there are 123 variables (columns) and 2,980 observations (rows) in the larger CSV file that we have archived at **dryad**, Young and Obenchain (August 2022), the analyses presented here actually use only the 11-variables described in Table 1 on page 4. These 11 variables are in the smaller CSV file in the same **dryad** archive that contains just 25 variables and 2,973 observations without any *missing values*. Six US Counties had NA codes on the rather important PREMdeath variable (FIPS = 8033, 30055, 31091, 46069, 46073 and 49031.) A 7<sup>th</sup> NA code occurred for FIPS = 32011 in the IncomIEQ variable, which turned out to be a relatively unimportant variable.

The analyses presented here will ultimately focus on “potential causes” of Circulatory and Respiratory Mortality within individual US Counties. Our focus on the AACRmort variable from the CDC (rather than CRmort) stems primarily from our previous experience [Obenchain, Young and Krstic (2019)] where the *proportion of county residents over 65* was a key predictor of local mortality. While we did perform some preliminary analyses using CRmort as the primary *y*-Outcome, we found them to be both more complex and less self-consistent than the corresponding AACRmort analyses that we present below.

Our somewhat surprising and unexpected findings concerning distinct components of pmTOT (i.e. PM<sub>2.5</sub>) focus primarily upon Bvoc, although the Avoc and pmSO4 variables from the EPA were also used in our final analyses.

TABLE 1 – Variable Information

Name	Description	Range	Source
FIPS	Federal Information Processing code (4 or 5 digits)	1001-56045	FED
CRmort	Crude Circulatory and/or Respiratory Mortality (per 100K)	64.8-1564	CDC
AACRmort	Age Adjusted Circulatory and/or Respiratory Mortality (per 100K)	95.5-802.6	CDC
pmTOT	Particles in Air with diameter less than 2.5 micrometres ( $\mu\text{g}/\text{m}^3$ )	2.06-14.32	EPA
Bvoc	(predicted) Biogenic Volatile Organic Compounds in pmTOT	0.26-3.31	EPA
Avoc	(predicted) Anthropogenic Volatile Organic Compounds in pmTOT	0.23-2.89	EPA
pmSO4	Sulfate Compounds in pmTOT	0.39-1.62	EPA
ASmoke	Adult Smoking Fraction	0.007-0.412	EPA
PREMdeath	Premature Death Rate	0.03-0.66	EPA
ChildPOV	Children Living in Poverty (per 100K)	2853-36469	EPA
IncomIEQ	Income In-Equality Rating	2.9-8.9	EPA

Although we ultimately focus on *Local* (within Cluster) models that are highly-flexible and statistically robust, an initial analysis of a simple linear (regression) model was used to assess the “overall” extent of ill-conditioning (confounding) among variables; see Figure 2 on page 5. This **Trace** display shows fitted regression coefficients for the *Efficient Generalized Ridge Regression* shrinkage path of Obenchain (2022). This linear model attempts to predict *AACRmort* using *Bvoc*, *Avoc*, *pmSO4*, *PREMdeath*, *ASmoke*, *ChildPOV* and *IncomIEQ*. While the order in which these seven “right-hand-side” variables are specified is irrelevant in classical linear regression, the first three are EPA environmental variables while the last four quantify socioeconomic characteristics of county residents.

### 3 Applying Local Control Strategy

While LC Strategy can be used by single researchers working alone, it may also be used by groups of collaborating researchers. In fact, LC Strategy may be an ideal approach for use when the researches involved in a collaboration have “odd combinations” of qualifications ...such as: diverse experiences and unique perspectives on the overall issues involved. Use of LC Strategy plus access to data then makes it possible to seriously address the question: Can any shared, consensus position be reached?

Our discussion of LC Strategy below will use the terminology introduced in Table 2, also on page 5.

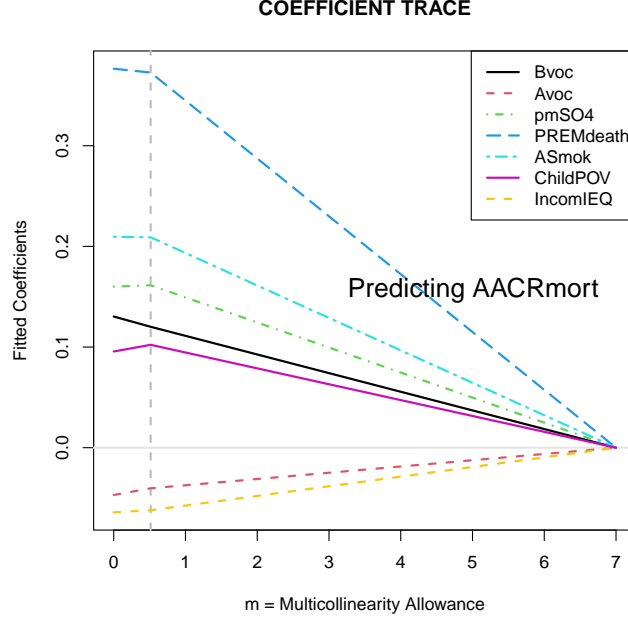


Figure 2: Following a modest initial extent of shrinkage to  $m = 0.51$ , MSE-risk optimal relative-magnitudes for  $\beta$ -coefficient estimates are determined. In other words, overall ill-conditioning (redundancy) among these seven  $X$ -variables appears minor. Since our main LC Strategy analyses will use AACRmort as the  $y$ -Outcome measure, we will focus on Bvoc as our primary (potentially causal) Exposure variable. After all, the EPA Avoc and IncomIEQ variables have only *small and negative coefficient estimates*. The genuinely “bad news” from this classical linear model is that its overall  $R^2$ -Coefficient of Determination is rather low (coincidentally, also 0.51). The “local” models developed here using LC Strategy will be non-linear, distribution-free and will provide much better fits.

**TABLE 2 – Basic LC Strategy Terminology**

Term	Description
Experimental Unit	An individual US County or Parish.
Cluster	A subgroup of Units that are relatively well-matched on their given $X$ -characteristics.
Cycle	One “pass” through the data involving at least the Aggregate and Confirm phases of analysis.
Aggregate Phase	The Phase of LC Strategy where new sets of Clusters are formed.
Confirm Phase	The Phase where a given Aggregation is shown to be either Ignorable or to provide Added Information.
Explore Phase	The Phase where Aggregations are ranked on Added Information and a decision of either Continue or Stop is made.
Reveal Phase	The final Phase of LC Strategy where the Variance-Bias Trade-Offs associated with the best Aggregation are Revealed and Discussed.

### 3.1 Forming the Hierarchical Clustering Tree

The first step in LC Strategy is to form a hierarchical clustering *dendrogram*. The `LocalControlStrategy::LCcluster()` function calls `stats::prcomp()` to calculate Mahalanobis distances using standardized and orthogonal Principal Coordinates, Obenchain (1971), Rubin (1980). These coordinates optimally quantify “dissimilarity” among US Counties using their possibly confounded  $X$ -characteristics. A dendrogram (tree-like structure) can usually be “cut” by a horizontal line to produce any desired number of individual clusters. Our dendrogram, displayed in Figure 3, uses the default “ward.D” clustering algorithm.

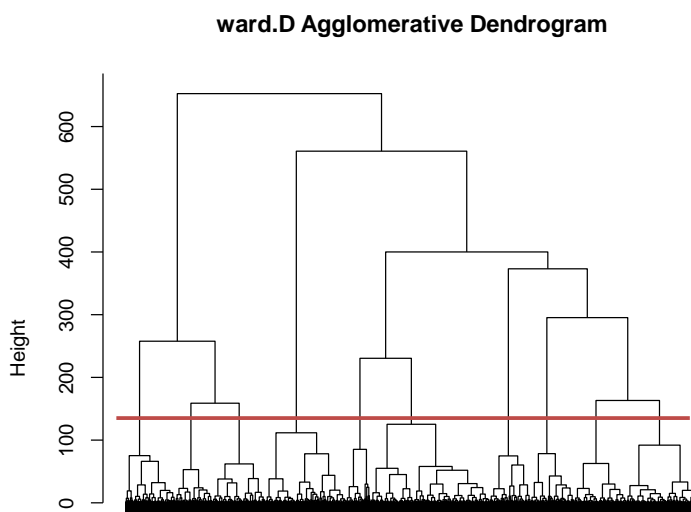


Figure 3: This Hierarchical Clustering **Dendrogram** can be “cut” by a horizontal line at any strictly positive Height. For example, note that the displayed red line produces 10 clusters.

Either the divisive `cluster::diana()` method or any of six agglomerative alternatives (`ward.D2`, `complete`, `average`, `mcquitty`, `median`, or `centroid`) could have been specified. However, “single-linkage” clustering is not appropriate for use in LC Strategy because it can produce clusters that are more like “strings” than like compact subgroups of most similar experimental units.

### 3.2 Confirming that a given Number of Clusters provide “Added Information”

Every new *Aggregate Phase* of LC Strategy is followed immediately by a *Confirm Phase* analysis asking whether the new “LRC distribution” could possibly be generated in some *Completely Random* way. Actually, it is easy to generate purely random LRC distributions that use both the same number of clusters and the same cluster sizes as any given “new” LRC distribution.

Figure 4 displays the numerical example with  $K = 50$  Clusters that we will use to illustrate *confirm phase testing*. We are “jumping the gun” here in the sense that we will argue next (Subsection 3.3) that  $K = 50$  is also the “optimal”

number of Clusters to use in applying LC Strategy.

LRC distributions are always discreet, while the traditional test that uses the Kolmogorov-Smirnov D-statistic is only valid for comparing two absolutely continuous distributions. Thus, LC Strategy uses a (computationally intensive) *permutation test*, Welch (1990), that is non-parametric. Specifically, the LC Strategy `confirm()` function easily simulates the gray eCDF displayed in Figure 4 and computes the resulting Kolmogorov-Smirnov D-statistic. These calculations take less than 5 seconds.

Note that the gray NULL eCDF appears to be rather *smooth* in Figure 4. After all, it results from pooling 100 sets of LRC estimates from 50 pseudo-clusters that were formed in a *purely random and meaningless way*. Thus the gray eCDF contains at most 5,000 quite small steps. To truly provide “added information”, the distribution underlying the Blue eCDF from clusters of “well matched” US Counties must be clearly different from the purely random distribution (from random pseudo-clusters) represented by the gray eCDF.

The primary objective of the `KSperm()` function in LC Strategy is to simulate an appropriate p-value, “adjusted” for ties, when testing the NULL hypothesis that all x-Covariates used to form clusters are essentially *Ignorable*. These computations, using 1,000 replications, take roughly 77 seconds on a desktop PC.

Figure 5 displays the NULL distribution where the *largest observed NULL D-statistic* is only 0.237. This simulated NULL D-statistic is dwarfed by the Observed *D*–statistic of 0.7903 in Figure 4. In other words, the Blue empirical CDF variable, named “LRC50”, provides abundant *Added Information* in the sense that it is clearly “shifted to the left” in Figure 4 relative to the simulated gray NULL eCDF. The Blue eCDF is thus *Not Ignorable*! Furthermore, note that some Local Rank Correlation estimates from  $K = 50$  clusters are *clearly negative*.

### 3.3 Choosing the Number of Clusters to Use in LC Strategy

Especially when cross-sectional data are observational, the data typically contain isolated “local” effects as well as overall (global) confounding from potentially highly correlated variables. The Nonparametric and Unsupervised “pre-processing” methods that characterize LC Strategy address these issues. Traditional methods based on multiple regression are typically Global, Parametric and Supervised. They tend to make much stronger (and possibly unrealistic) assumptions that yield questionable global predictions and potential extrapolations.

In sharp contrast, LC Strategy summarizes findings from several separate and flexible “local” models that are fit within *clusters of “most similar” and/or relatively “well-matched” experimental units*. The number of such local models and separate clusters of experimental units being used in a given Cycle is denoted by the symbol **K**.

LC Strategy embraces many of the basic concepts and experiences outlined in Stuart (2010), van der Laan and Rose (2010) and Stang et al. (2010). Published analyses using LC Strategy include: Obenchain and Young (2013); Lopiano, Obenchain and Young(2014); Young, Smith and Lopiano (2017) and Obenchain, Young and Krstic (2019).

The LC approach consists of Four Phases of analysis called, respectively : *Aggregate*, *Confirm*, *Explore* and *Reveal*. Each analysis “cycle” through the available data typically uses a different Aggregation of experimental units into a larger and larger number,  $K$ , of smaller and smaller “Clusters”. Potential results from each new cycle are then either discarded or else *Confirmed* to provide *Added Information* ...in the sense of being clearly different from “purely random” in ways discussed below.

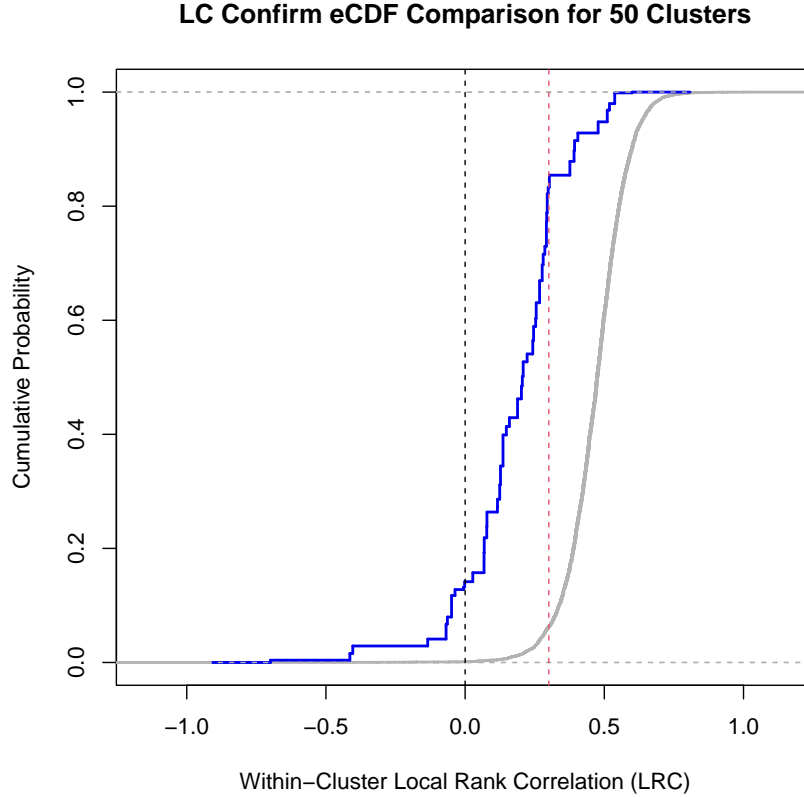


Figure 4: This plot displays a pair of empirical Cumulative Distribution Functions (eCDFs) and addresses the question of whether they are statistically different. Note that the Kolmogorov-Smirnov D-statistic of 0.7903 (maximum vertical separation between eCDFs) occurs here at 0.30 on the horizontal axis ...marked by the dashed red line.

The implicit statistical model used in LC Strategy is simply one-way ANOVA. The Within-Block measures of effect-size when the  $e$ -variable is an Exposure (with many more than just two levels) are “Local Rank Correlations” (LRCs) between Exposures and  $y$ -Outcomes. A single cluster containing  $N$  US Counties thus contributes  $N$  identical LRC estimates to the overall (across cluster) distribution of LRC “effect-sizes”.

Ultimately, we chose to use  $K = 50$  Clusters of US Counties formed using only 6-Key  $X$ -confounder variables, out of the more than 100 that were available. These 50 clusters represent mutually exclusive and exhaustive statistical “Blocks” of *relatively well-matched experimental units*, and our resulting “best” Effect-Size distribution quantifies a potentially causal relationship between the numeric  $y$ -Outcome variable AACRmort and the  $e$ -Exposure variable Bvoc.

Our choice of  $K = 50$  clusters was determined within the *Explore* phase when *Box - Plots* showed that the



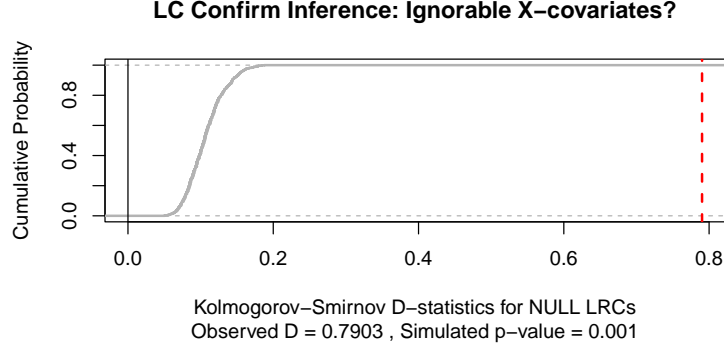


Figure 5: Since the traditional Kolmogorov-Smirnov test compares eCDFs from a pair of *Continuous Distributions*, it is severely biased when used to compare *Discrete Distributions*. Thus, simulation is used in LC Strategy to make valid comparisons between eCDF estimates. Since the largest observed NULL D-statistic was only 0.237, the Observed D of 0.7903 almost surely has an actual  $p$ -Value of **much less than** 0.001 (one in a thousand).

distribution of estimated “effect sizes” would become excessively variable for  $K > 50$ . Specifically, any analyst applying *LC Strategy* would examine the “LCcompare()” graphic displayed in Figure 6 on page 10 and choose  $K = 50$  for the very reasons outlined in the caption of that figure.

## 4 LC “Reveal” Stage: randomForests, Partial Dependence Plots and a Single RP Tree

We can now stop our “Explore” phase analyses and enter a (final) “Reveal” phase. Specifically, we now look across, rather than only within, the  $K = 50$  clusters of relatively well-matched US Counties that provide the most (potentially causal) *Added Information* about relationships between the AACRmort and Bvoc “measures” of mortality and air pollution, respectively. This new information is embedded within the LRC50 variable that takes on only one of 50 distinct numerical values between  $-0.699$  and  $+0.600$  for each US County.

### 4.1 Interaction Effects Abound

Figure 9 contains plots of Bvoc versus AACRmort for 4 of our 50 Clusters. The two left-hand clusters have positive LRC-estimates and blue least-squares lines that slope upwards, while the two right-hand clusters have negative LRC-estimates and blue least-squares lines that slope downwards. Actually, 421 US Counties (21.3%) of all 2,973 US Counties without missing data fall into the 10 out of 50 Clusters (i.e. 20%) that yield *negative LRC-estimates*. In other words, almost 80% of US Counties are in the 80% of Clusters with strictly positive LRC-estimates. After all, the Rank-Correlation for the overall Bvoc vs. AACRmort scatter displayed in Figure 1 is  $+0.474$ . This made us

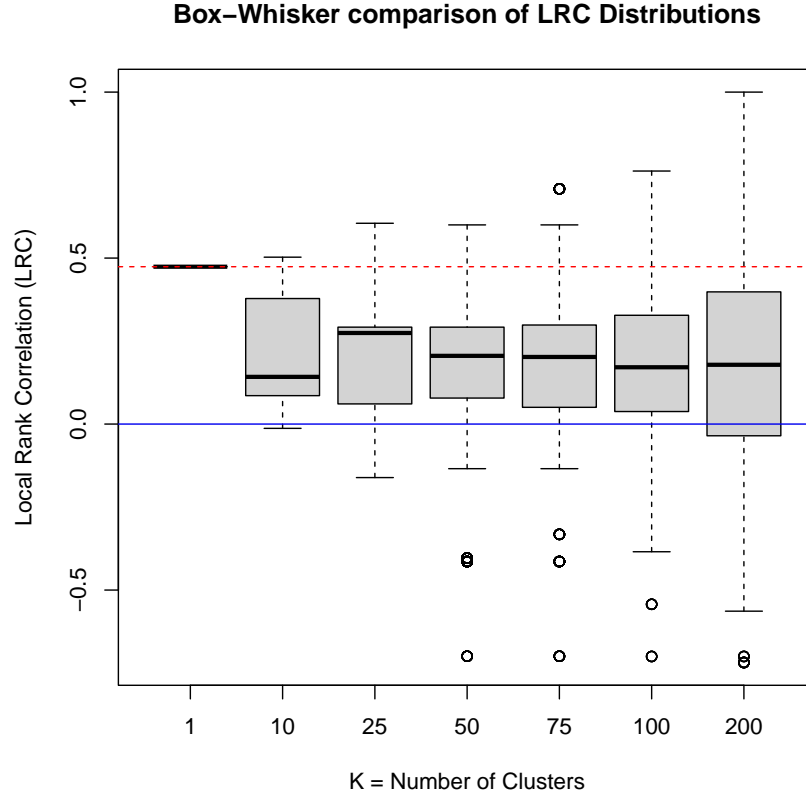


Figure 6: Here we see 7 I-plots of the overall distribution of LRC effect-sizes as the number of clusters,  $K$ , being formed increases from 1 to 200. Note that there is clear evidence that Variance–Bias Trade–Offs are occurring for  $K \geq 50$ . For example, the Vertical inter-quartile ranges of local distributions then steadily increase, and the median of local effect–sizes is minimized at  $K = 100$ . However, the vertical spread between upper and lower extremes of LRC distributions start becoming excessive for  $K > 50$ . Our recommended “compromise” choice is thus  $K = 50$ .

wonder whether larger clusters might tend to produce positive LRC estimates?

An extreme illustration of this is displayed in the lower-right panel of Figure 10. Data from the 237 Counties within the 6 clusters with the most Negative LRCs are merged together there, yielding a scatter with clearly positive slope (and an LRC of +0.267.) Meanwhile, each of the other 3 panels shows scatters for 2 out of the 6 clusters with most negative LRCs. Clearly, clustering of US Counties on their confounded  $X$ –characteristics predictive of AACRMort *truly does matter*!

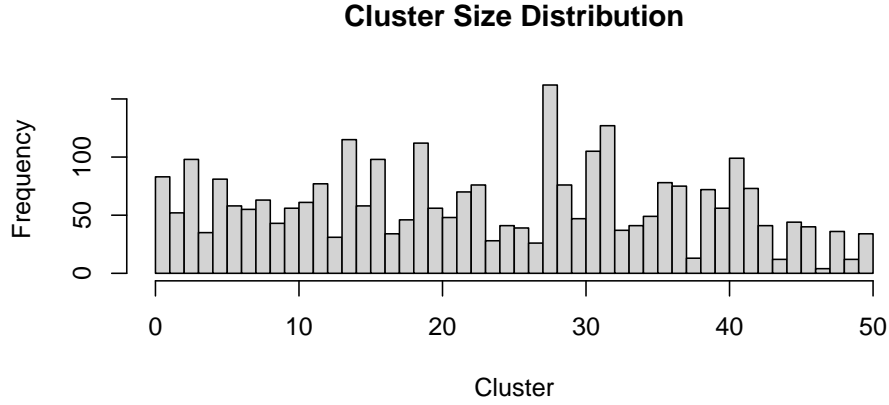


Figure 7: This histogram shows the number of US Counties within each of the 50 Clusters formed using observational data from the EPA, CDC and US Census. In a prospective study (e.g. a well “designed” experiment), all “blocks” of well-matched experimental units are usually of nearly equal size. But that’s an unlikely “ideal” situation when analyses must rely on observational data.

## 4.2 Insights from a randomForest of 500 Trees

The highly detailed captions for the next eight Figures (11 through 18) outline our interpretations of the relationships revealed by Partial Dependence Plots (PDPs) within our “randomForest” of 500 tree models.

Table 3 summarizes the key characteristics of our eight PDP plots. The top 4  $X$ -confounder variables predictive of AACRmort include the three variables inducing highest Incremental Node Purity.

**TABLE 3 – Importance Statistics for 8 Variables**

Variable	%IncMSE	IncNodePurity
ASmoke	71.28070	16.611216
ChildPOV	59.45606	17.160771
PREMdeath	56.31122	11.765453
Bvoc	46.40073	16.198999
pmSO4	37.81722	12.071959
Avoc	25.25779	14.658269
AACRmort	17.79182	4.878167
IncomIEQ	16.14760	5.173446

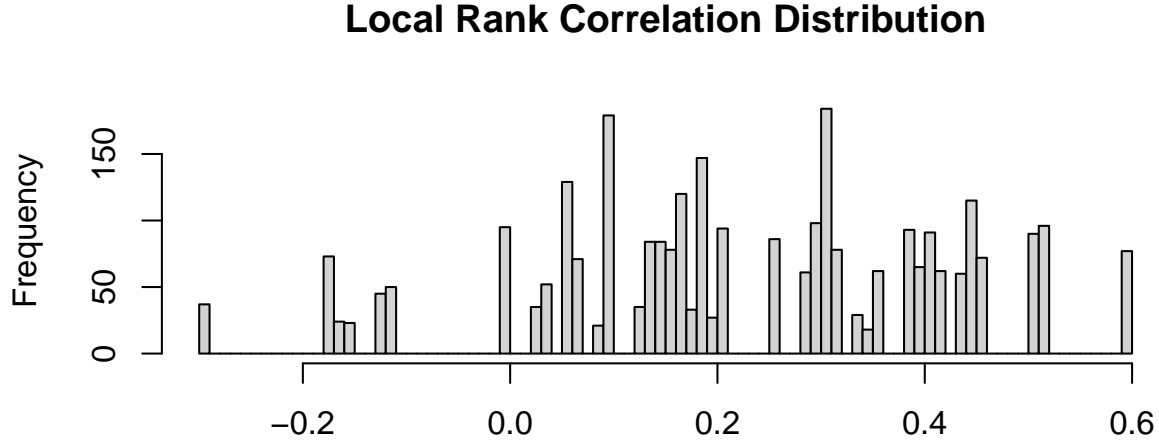


Figure 8: Here we see that the distribution of Local Rank Correlations (LRCs) within our 50 Clusters spans the range from  $-0.30$  to  $+0.60$ . Since this distribution contains only 50 distinct numerical values, it certainly does not (and cannot) look much like a “continuous” parametric distribution.

### 4.3 Insights from Model-Based Recursive Partitioning

We used the “model based” algorithms of Zeileis, Hothorn and Hornik (2008) to develop the single Recursive Partitioning tree displayed in Figure 19. Note that this approach searches for “optimal intervals” of Bvoc values within which observed LRCs can be predicted from local ASmoke levels using simple linear regression. Summary statistics for the 7 Bvoc intervals that resulted are listed in Table 4 on page 18.

## 5 Summary

Personal computers have helped shape statistical theory as well as its practice over the last 50 years. Freely available software can provide computational and visual fast-tracks into the strengths and weaknesses of alternative statistical methods. For example, the lower right-hand panel of Figure 10 showed just how misleading a scatter-plot can be that ignores cluster-membership. Our clusters contain US Counties with most similar  $X$ —characteristics, so they compare only “apples” with “apples”, “potatoes” with “potatoes”, etc, etc. This strategy leads to either *fair comparisons* when the exposure variable is binary [Lopiano, Obenchain and Young (2014)], or to *cogent local inferences* when that exposure (Bvoc) is both continuous and correlated with potential confounding variables (Avoc, pmSO<sub>4</sub>, ChildPOV, etc, etc.)

The eight PDP plots that are displayed in Figures 10 to 17 and summarized in Table 3 on page 14 have encouraged us to focus our attention primarily on the top-four predictors of LRCs; Bvoc is number four. Unfortunately, neither

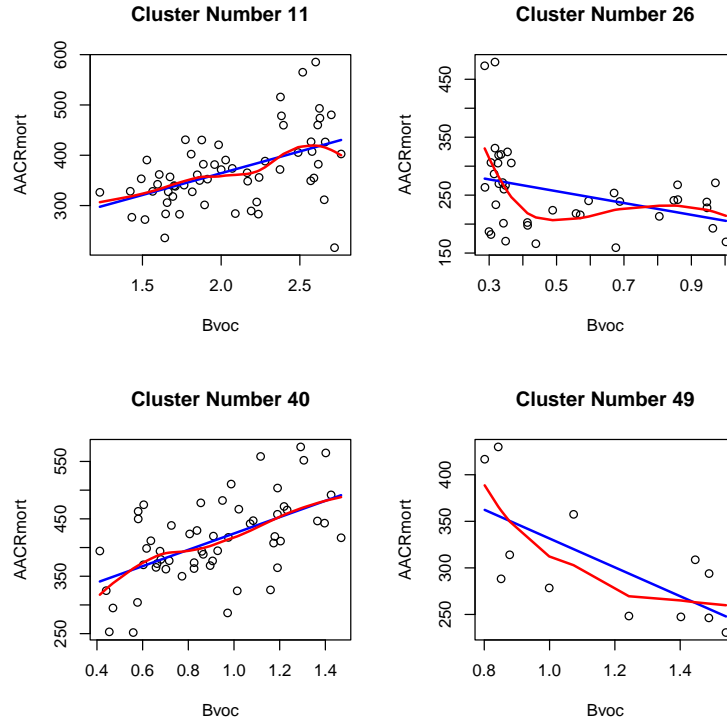


Figure 9: Here are plots of Bvoc versus AACRmort within four of the 50 Clusters. The straight blue lines are least-squares fits, while the red curves are “loess” smooths (span = 0.75) for predicting AACRmort from Bvoc. While the (Spearman) LRCs within the two left-hand Clusters (11 and 40) are positive, both right-hand clusters (26 and 49) are typical of the negative LRC estimates observed for a total of 421 US Counties (21.3% of the 2,973 US Counties without missing data).

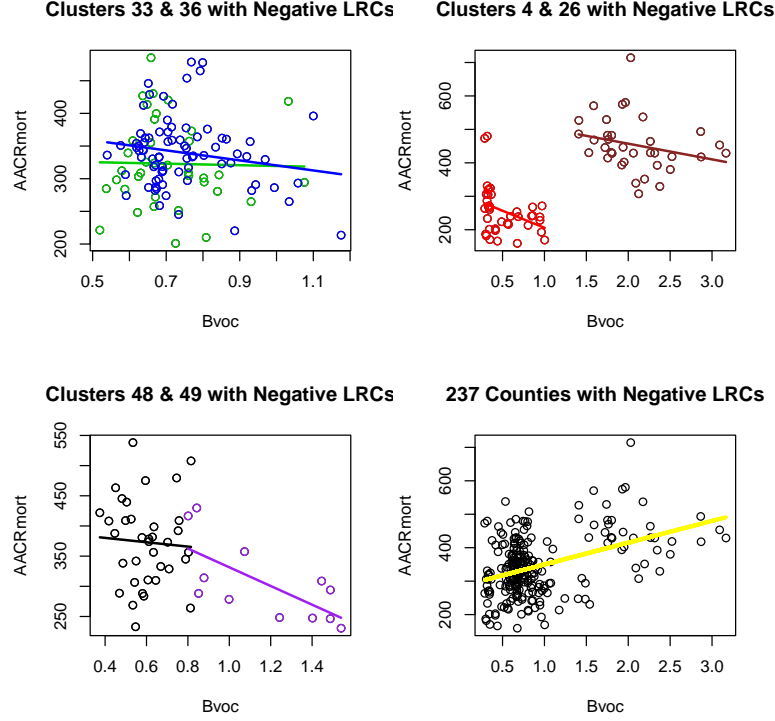


Figure 10: When AACRmort and Bvoc data from the 6 clusters with most Negative LRC estimates are merged together, much of their cluster “identity” gets lost. This is clear in the lower-right panel: their “merged trend” is then clearly Positive (shown in Yellow). Each of the other three panels show AACRmort vs. Bvoc scatters for two clusters with negative LRCs using a total of six different colors.

$pmSOA \equiv Avoc + Bvoc$  nor either of its two components can apparently be actually “measured” today ...using existing scientific instruments with reasonable accuracy.

Bvocs include *Terpenes* from trees and grass, and EPA Bvoc *predictions* are, at least on average, positively correlated with corresponding local CDC CRmort counts, before and after being Age Adjusted. How will US environmentalists react to this “news”? Luckily, our single RP tree in Figure 19 does suggest that levels of Bvoc  $> 1.01$  can be protective against high AACRmort when ASmoke rates are above roughly 20%.

The future of NU-Learning approaches for analysis of cross-sectional observational data strikes us as being quite promising. Unfortunately, traditional (Parametric and Supervised Learning) models used in Propensity Score estimation tend to be global (rather than local) and may make strong and potentially unrealistic assumptions.

Most interesting questions don’t have an answer that is clearly “Black” or “White”. Data from well-designed and well-executed experiments can illuminate some key issues. Meanwhile, large collections of observational data can reveal interesting real-world “shades of gray”.

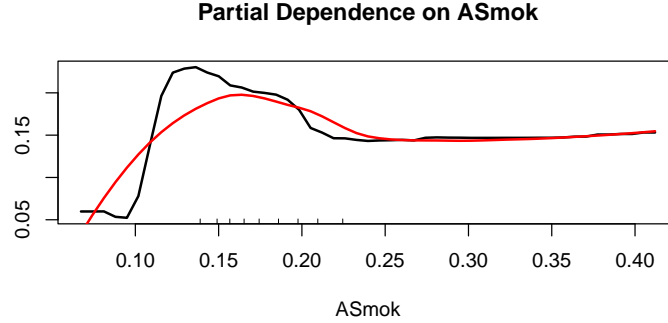


Figure 11: The single most important predictor of LRCs is ASmoke (%IncMSE= 71.28). Adult Smoking rates within the .15 to .20 range are most predictive of positive LRCs between AACRmort and Bvoc. For some unknown reason, smoking rates above .25 correspond to somewhat lower but still relatively high LRCs.

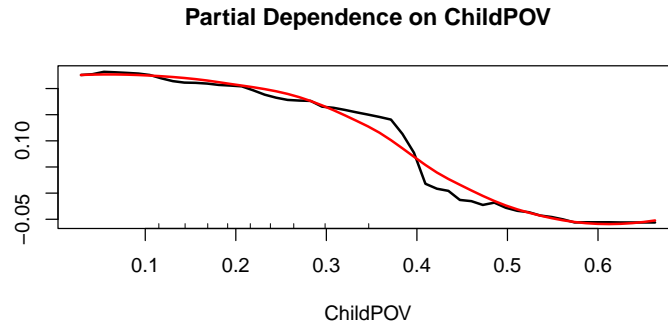


Figure 12: The second most important predictor of LRCs is ChildPOV (%IncMSE= 59.46). When Children in Poverty rates are less than .30, LRCs are strongly positive. But LRCs then drop and can be negative when ChildPOV  $\geq .50$ . In fact, ChildPOV is the only predictor associated with strictly negative LRC predictions ...where AACRmort counts tend to decrease as Bvoc levels increase.

Our use of LC Strategy in our analysis of rather voluminous and detailed data highlights a truly key advantage of our computer intensive approach. Namely, this approach generates many simple yet highly informative graphical displays that range from simplistic to quite detailed. Using a wide variety of displays can guide further analyses in unanticipated directions. For example, note the great detail embedded within Figures 19 through 22. Using a PDF reader with Adobe zoom capability enables comparisons among US counties that are “similar” in terms of either *Cluster Membership* in seven dimensions (Bvoc, Avoc, pmSO<sub>4</sub>, PREMdeath, ASmoke, ChildPOV and IncomIEQ) or *Geography* in two dimensions (lat and long).

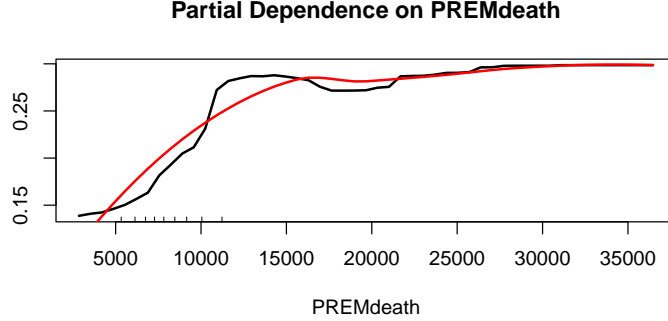


Figure 13: The third most important predictor of LRCs is PREMdeath (%IncMSE= 56.31). PREMdeath is the (raw) count of premature deaths per 100,000 county residents. As this rate increases from 5,000 to 15,000, LRCs steadily increase from 0.15 to about 0.28. LRCs then approach 0.30 for all PREMdeath counts exceeding 20,000. A high PREMdeath count appears to be a truly insidious indicator of poor Circulatory and/or Respiratory Health.

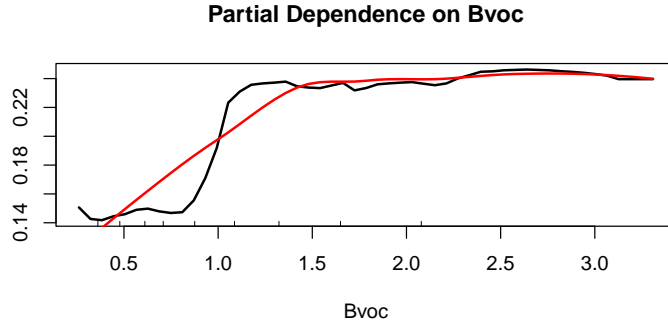


Figure 14: The fourth most important predictor of LRCs (Within-Cluster Spearman rank correlations between AACRmort and Bvoc) is Bvoc itself (%IncMSE= 46.40). As local Bvoc levels increase from 0.2 to 1.5, LRCs tend to steadily increase from 0.15 to a maximum of 0.24 and remain at this highest level for further increases in Bvoc level.

Our main contributions and forward-looking recommendations are:

- (1.) We have made CSV files publicly available that contain data as much “like” the CDC and EPS data used by Pye et al. (2021) as is possible by private US citizens.
- (2.) Use of *LC Strategy* in our analyses of these data has yielded findings that are fundamentally different and quite possibly more relevant and technically sound than those of Pye et al. (2021). Since interaction effects abound within the data, it’s not surprising that local models provide better fits than “smoothly” continuous global models.
- (3.) It became clear in our earliest data analyses that Bvoc would be a better predictor of AACRmort than Avoc



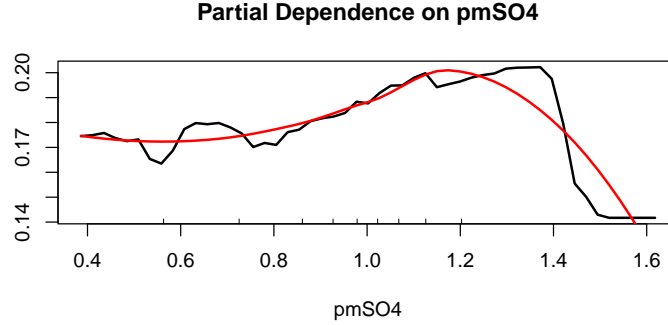


Figure 15: The fifth important predictor of LRCs is  $pmSO_4$  (%IncMSE= 37.82). This PDPlot suggests, curiously, that, while LRCs steadily increase over the range  $0.4 - 1.4$ , they sharply drop when  $pmSO_4$  exceeds 1.4.

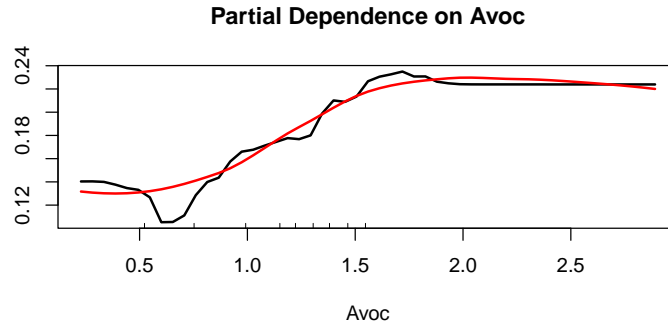


Figure 16: The sixth important predictor of LRCs is  $Avoc$  (%IncMSE= 25.26). Here, LRCs tend to mostly increase from about 0.12 to 0.20 over the initial range of  $0.1 \leq Avoc \leq 1.5$ , then remain above 0.22 when  $Avoc$  exceeds 1.8. The general shape of this PDP is somewhat like that for the  $Bvoc$  predictor, Figure 14.

or  $pmSOA \equiv Avoc + Bvoc$ . For example, the (Pearson) correlation  $cor(AACRmort, Bvoc) = 0.4589$  is larger than both  $cor(AACRmort, Avoc) = 0.2489$  and  $cor(AACRmort, pmSOA) = 0.4253$ . Furthermore, all  $Avoc$   $\beta$ -coefficient estimates are *negative* in Figure 2. Did Pye et al. (2021) avoid talking about  $Bvoc$  effects primarily because EPA regulation of  $Bvoc$  would have no clear organization to hold responsible?

(4.) What, exactly, is the EPA explanation of why their CMAQ models (2019) appear to be much better predictors of  $AACRmort$  (or  $CRmort$  before Age Adjustment) than models from academic research traditionally funded by the EPA? For example, does CMAQ use information on variation in socioeconomic characteristics of residents? How and when will  $pmSOA$  and its components become accurately measurable? We recommend considerable skepticism while waiting for answers to these sorts of questions!

**TABLE 4 – Statistics for LRC Prediction within 7 Bvoc Intervals**

Final Node	LRC Intercept	ASmoke Slope	Bvoc Range	Bvoc Level	US Counties
4	-0.00411	+1.09902	$\leq 0.313$	Low	126
5	-0.13183	+1.42106	0.313-0.439	Low	379
====	====	====	====	====	====
7	0.33623	-1.24350	0.439-0.805	Medium	862
8	0.12447	+0.29020	0.805-1.010	Medium	323
====	====	====	====	====	====
10	0.45914	-1.01360	1.010-1.718	High	750
12	0.86823	-3.21152	1.718-2.237	High	311
13	1.31711	-5.09834	$> 2.237$	High	222

## R-code and Data Availability

A file named *LCSonEPA.Code.pdf* can be freely downloaded from <http://localcontrolstatistics.org>. This PDF contains all R-code needed to perform the analyses and display example figures. A variety of introductory information about **LC Strategy** can also be freely downloaded from this internet site.

Our reconstruction of all 123 variables used by Pye et al. (2021) can be downloaded from <https://datadryad.org>. We merged files from the CDC and EPA using FIPS codes and created CSV files with shorter variable names. The larger “CDC.EPA.2022.csv” file contains 123 variables while “AnalysisFile.csv” contains only the 25 variables either considered for or actually used in the analyses presented in this paper. The smaller file contains data on 2,973 US Counties without “missing values”, while the larger file contains everything in the smaller file, except the Cluster membership number and LRC value, for 2,980 US Counties.

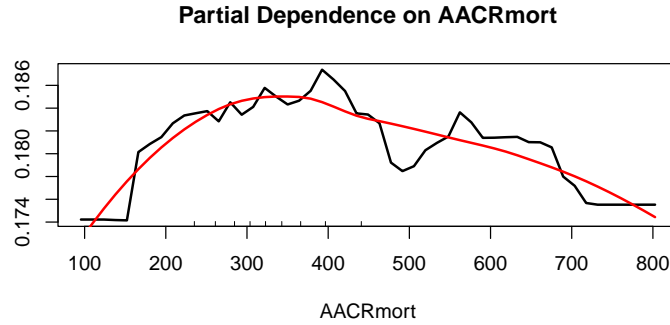


Figure 17: A seventh predictor of LRCs (between AACRmort and Bvoc) is AACRmort itself: %IncMSE= 17.79. Since the vertical range in this plot is quite small (0.014), any suggestion of “curvature” here is relatively unimportant.

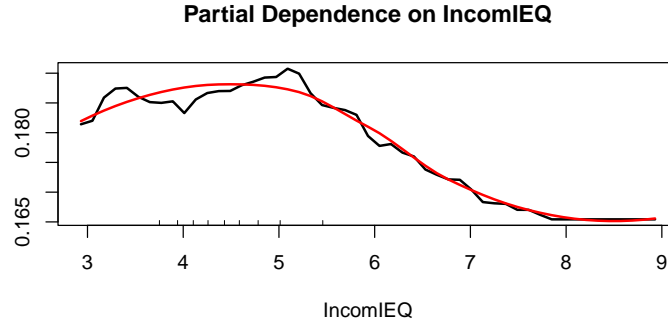


Figure 18: The last (and least important) predictor of within-cluster LRCs is IncomIEQ %IncMSE= 16.15. LRCs tend to be near to 0.185 for  $3 \leq \text{IncomIEQ} \leq 5.5$ , then steadily drop to 0.165 for IncomIEQ above 8.

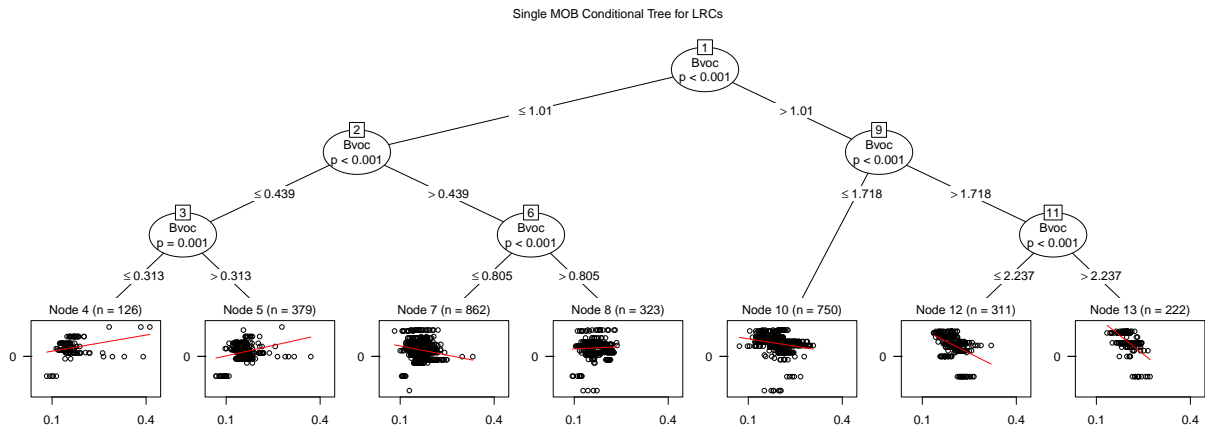


Figure 19: This figure suggests that high ASmoke rates are particularly harmful within the two lowest Bvoc intervals. Within four of the five higher Bvoc intervals towards the right, LRCs (between AACRmort and Bvoc) are surprisingly predicted to decrease as local ASmoke rates increase.

## Conflict of Interest

The authors state no conflicts of interest.

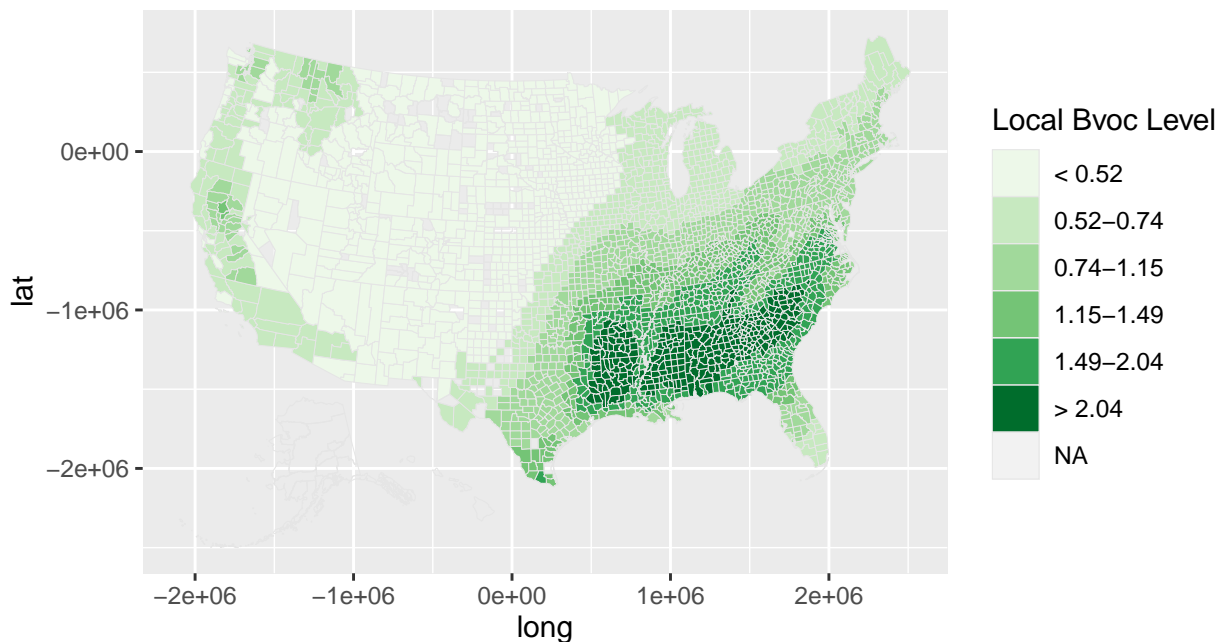


Figure 20: This US map, Kahle and Wickham (2013), shows variation in EPA Bvoc predictions across US Counties using six shades of Green. Low Bvoc levels receiving the lightest shade of Green dominate the US “Great Plains” and Rocky Mountain regions where agricultural production is either low or supported by irrigation. Note that a vast majority of counties receive the same Bvoc color as their adjacent counties. Note also that 151 US Counties fall into the 7<sup>th</sup> “NA” category and receive the see-through “background” color.

## References

- [1] Breiman, L. (2001), “*Random Forests*”, Machine Learning, 45, 5–32. <https://doi.org/10.1023/A:1010933404324>.
- [2] Breiman, L. (2002), “*Manual On Setting Up, Using, And Understanding Random Forests, V3.1*”. [https://www.stat.berkeley.edu/~breiman/Using\\_random\\_forests\\_V3.1.pdf](https://www.stat.berkeley.edu/~breiman/Using_random_forests_V3.1.pdf).
- [3] Centers for Disease Control and Prevention National Center for Health Statistics. Compressed Mortality File 1999-2016 on CDC WONDER Online Database, released June 2017. Data are from the Compressed Mortality File 1999-2016 Series 20 No.2U, 2016, as compiled from data provided by the 7 vital statistics jurisdictions through the Vital Statistics Cooperative Program. Accessed by Obenchain on 19 April 2022, <http://wonder.cdc.gov/cmfi-icd10.html>.

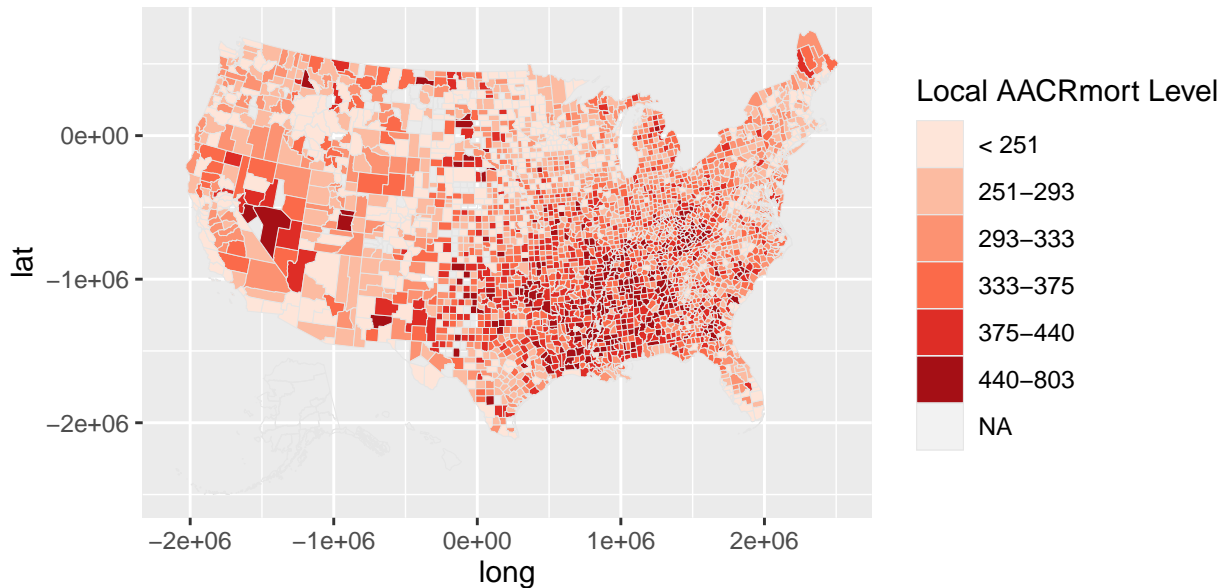


Figure 21: This map shows variation in AACRmort counts per 100,000 residents using six shades of Red. These adjusted counts are certainly not smooth functions of geographic latitude and longitude; variation in AACRmort counts may result primarily from variation in the socioeconomic characteristics of local residents. After all, the vast majority of adjacent counties receive a somewhat different or very different shade of Red.

- [4] Friedman, J. (2001), “*Greedy function approximation: the gradient boosting machine*”, Annals of Statistics, 29(5), 1189–1232, <https://doi.org/10.1214/aos/1013203451>.
- [5] Glaeser, E.L. (2006), “*Researcher incentives and empirical methods*”, [https://www.nber.org/system/files/working\\_papers/t0329/t0329.pdf](https://www.nber.org/system/files/working_papers/t0329/t0329.pdf).
- [6] Hothorn, T. and Zeileis, A. (2015), “*partykit: A Modular Toolkit for Recursive Partytioning in R.*”, Journal of Machine Learning Research, 16, 3905–3909. <https://jmlr.org/papers/v16/hothorn15a.html>.
- [7] Hothorn, T., Seibold, H. and Zeileis, A. (2015-2022), “*partykit: A Modular Toolkit for Recursive Partytioning*”, ver 1.2-16, <https://CRAN.R-project.org/package=partykit>.
- [8] Kahle, D. and Wickham, H. (2013), “*ggmap: Spatial Visualization with ggplot2.*”, The R Journal, 5, 144–161. <http://journal.r-project.org/archive/2013-1/kahle-wickham.pdf>.
- [9] Koenker, R. (2005 - 2022), “*quantreg: Quantile Regression*”, ver 5.94, <https://CRAN.R-project.org/package=quantreg>.

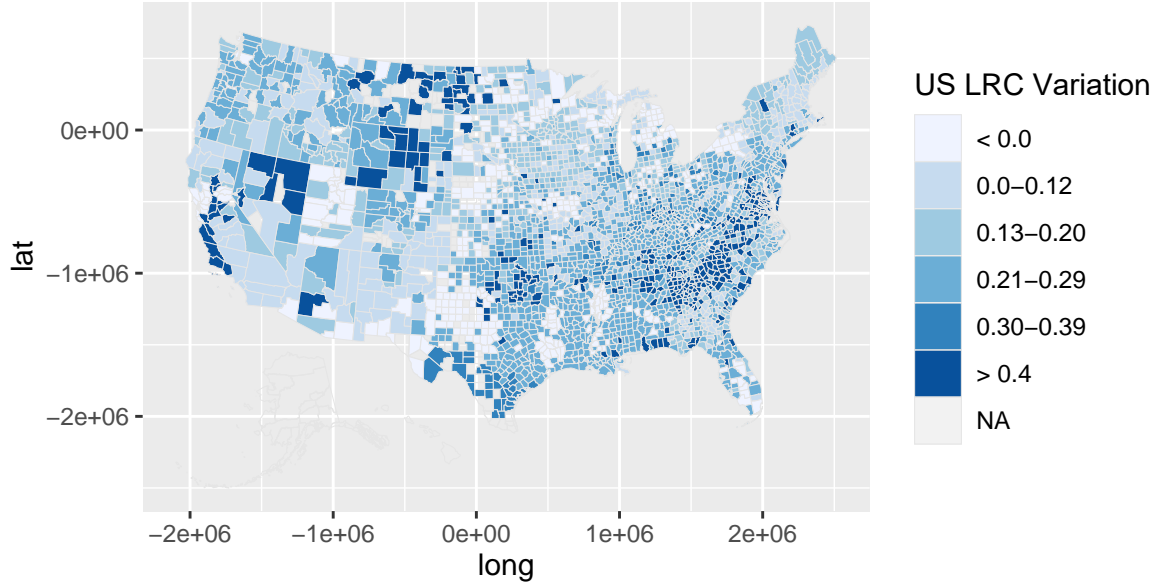


Figure 22: On this map showing variation in *Local Rank Correlations (LRCs)* across US Counties, six shades of Blue identify LRC levels of association between AACRMort and Bvoc within our 50 clusters of US counties well-matched in the 7-dimensional space of potential confounded characteristics. Note that all adjacent counties receiving different shades of Blue must be in different Clusters and thus have somewhat different characteristics. All 421 counties with negative LRC estimates receive the lightest shade of Blue. Again, 151 counties without data receive the see-through “background” color.

- [10] Liaw, A. and Wiener, M. (2002 - 2022) “*randomForest*: Breiman and Cutler’s Random Forests for Classification and Regression”, ver 4.7-1, <https://CRAN.R-project.org/package=randomForest>.
- [11] Lopiano, K.K., Obenchain, R.L. and Young, S.S. (2014), “*Fair Treatment Comparisons in Observational Research*”, *Statistical Analysis and Data Mining*, 7, 376–384. <https://doi.org/10.1002/sam.11235>.
- [12] Obenchain, R.L. (1971), “*Multivariate Procedures Invariant under Linear Transformations*”, *Annals of Mathematical Statistics*, 42: 1569–1578. <https://doi.org/10.1214/aoms/1177693155>.
- [13] Obenchain, R.L. (2005-2022), “*RXshrink*: Maximum Likelihood Shrinkage using Generalized Ridge or Least Angle Regression Methods”, ver 2.1, <https://CRAN.R-project.org/package=RXshrink>.
- [14] Obenchain, R.L. (2015-2019), “*LocalControlStrategy*: Local Control Strategy for Robust Analysis of Cross-Sectional Data”, ver 1.3.3, <https://CRAN.R-project.org/package=LocalControlStrategy>.

- [15] Obenchain, R.L. (2022), “*Efficient Generalized Ridge Regression*”, Open Statistics, 3: 1–18. <https://doi.org/10.1515/stat-2022-0108>.
- [16] Obenchain, R.L. and Young, S.S. (2013), “*Advancing statistical thinking in health care research*”, Journal of Statistical Theory and Practice, 7, 456–469. <https://doi.org/10.1080/15598608.2013.772821>.
- [17] Obenchain, R.L., Young, S.S. and Krstic, G. (2019), “*Low-level Radon Exposure and Lung Cancer Mortality*”, Regulatory Toxicology and Pharmacology, 107, <https://doi.org/10.1016/j.yrtph.2019.104418>.
- [18] Pye, H.O.T., Ward-Caviness, C.K., Murphy, B.N., Appel, K.W. and Seltzer, K.M. (2021), “*Secondary organic aerosol association with cardiorespiratory disease mortality in the United States*”. Nature Communications 12, 7215. <https://doi.org/10.1038/s41467-021-27484-1>.
- [19] R Core Team. (2022), “*R: A language and environment for statistical computing*”. <https://www.R-project.org/>
- [20] Rubin, D.B. (1980), “*Bias reduction using Mahalanobis metric matching*”. Biometrics, 36, 293–298. <https://www.jstor.org/stable/2529981>.
- [21] Stang, P.E., Ryan, P.B., Racoosin, J.A., Overhage, J.M., Hartzema, A.G., Reich, C., Welebob, E., Scarnecchia, T. and Woodcock, J. (2010), “*Advancing the Science for Active Surveillance: Rationale and Design for the Observational Medical Outcomes Partnership*”. Annals of Internal Medicine, 153, 600–606. <https://doi.org/10.7326/0003-4819-153-9-201011020-00010>.
- [22] Stuart, E.A. (2010), “*Matching methods for causal inference: A review and a look forward*”. Statistical Science, 25, 1–21. <https://doi.org/10.1214/09-STS313>.
- [23] U.S. EPA Office of Research and Development. (2019), “*CMAQ (Version 5.3.1)*”, <https://doi.org/10.5281/zenodo.3585898>.
- [24] Volkamer, R., Jimenez, J.L., San Martini, F., Dzepina, K., Qi, Z., Salcedo, D., Molina, L.T., Worsnop, D.R. and Molina, M.J. (2006), “*Secondary organic aerosol formation from anthropogenic air pollution: Rapid and higher than expected*”. Geophys. Res. Lett. <https://doi.org/10.1029/2006GL026899>.
- [25] Welch, W.J. (1990), “*Construction of permutation tests.*” Journal American Statistical Association, 85, 693–698. <https://doi.org/10.1080/01621459.1990.10474929>.
- [26] Wickham, H. (2016), “*ggplot2: Elegant Graphics for Data Analysis*”. New York: Springer-Verlag.
- [27] Wood, S. N. (2003), “*Thin plate regression splines*”. J. R. Stat. Soc. B. Met. 65, 95–114. <https://doi.org/10.1111/1467-9868.00374>.
- [28] Wood, S. N. (2004), “*Stable and efficient multiple smoothing parameter estimation for generalized additive models*”. Journal American Statistical Association, 99, 673–686. <https://doi.org/10.1198/016214504000000980>

- [29] Wood, S. N. (2022), “*mgcv*: Mixed GAM Computation Vehicle with Automatic Smoothness Estimation”, <https://CRAN.R-project.org/package=mgcv>.
- [30] van der Laan, M. and Rose, S. (2010), “*Statistics ready for a revolution: Next generation of statisticians must build tools for massive data sets*”. AMStat News, September, 38–39. <https://magazine.amstat.org/blog/2010/09/01/statrevolution/>.
- [31] Young, S.S., Kindzierski, W. and Randall, D. (May 2021), “*Shifting Sands: Unsound Science and Unsafe Regulation. Report #1: Keeping Count of Government Science – P-Value Plotting, P-Hacking, and PM2.5 Regulation*”. National Association of Scholars. <https://files.eric.ed.gov/fulltext/ED616199.pdf>.
- [32] Young, S.S., Obenchain, R.L. (August 2022), “*EPA Particulate Matter Data*”. <https://doi.org/10.5061/dryad.63xsj3v58>.
- [33] Young, S.S., Smith, R.L. and Lopiano, K.K. (2017), “*Air Quality and Acute Deaths in California, 2000–2012*”, Regulatory Toxicology and Pharmacology, 88, 173–184. <https://doi.org/10.1016/j.yrtph.2017.06.003>.
- [34] Zeileis, A., Hothorn, T. and Hornik, K. (2008). “Model-Based Recursive Partitioning.” *Journal of Computational and Graphical Statistics*, 17, 492–514. <https://doi.org/10.1198/106186008X319331>.